Fibroblast Activation Protein Targeted Therapy Using [^{177}Lu]FAPI-46 Compared with [^{225}Ac]FAPI-46 in a Pancreatic Cancer Model

Yuwei Liu (liuyuwei19930720@gmail.com)
Department of Nuclear Medicine and Tracer Kinetics, Graduate School of Medicine, Osaka University
https://orcid.org/0000-0003-0762-9840

Tadashi Watabe
Department of Nuclear Medicine and Tracer Kinetics, Graduate School of Medicine, Osaka University

Kazuko Kaneda-Nakashima
Institute for Radiation Sciences, Osaka University

Yoshifumi Shirakami
Institute for Radiation Sciences, Osaka University

Sadahiro Naka
Department of Radiology, Osaka University Hospital

Kazuhiro Ooe
Department of Nuclear Medicine and Tracer Kinetics, Graduate School of Medicine, Osaka University

Atsushi Toyoshima
Institute for Radiation Sciences, Osaka University

Kojiro Nagata
Radioisotope Research Center, Institute for Radiation Sciences, Osaka University

Uwe Haberkorn
Department of Nuclear Medicine, University Hospital Heidlberg

Clemens Kratochwil
Department of Nuclear Medicine, University Hospital Heidelberg

Atsushi Shinohara
Department of Chemistry, Graduate School of Science, Osaka University

Jun Hatazawa
Research Center for Nuclear Physics, Osaka University

Frederik Giesel
Department of Nuclear Medicine, University Hospital Heidelberg

Research Article

Keywords: fibroblast activation protein, pancreatic cancer, FAPI, lutetium, actinium

Posted Date: June 17th, 2021

DOI: https://doi.org/10.21203/rs.3.rs-602564/v1

Version of Record: A version of this preprint was published at European Journal of Nuclear Medicine and Molecular Imaging on September 18th, 2021. See the published version at https://doi.org/10.1007/s00259-021-05554-2.

Abstract

Purpose

Fibroblast activation protein (FAP), which has high expression in cancer-associated fibroblasts of epithelial cancers, can be used as a theranostic target. Our previous study used ^{64}Cu and ^{225}Ac-labelled FAP inhibitors (FAPI-04) for a FAP-expressing pancreatic cancer xenograft imaging and therapy. However, the optimal therapeutic radionuclide for FAPI still needs to be further investigated. In this study, we evaluated the therapeutic effects of beta-emitter(^{177}Lu)-labelled FAPI-46 and alpha-emitter(^{225}Ac)-labelled FAPI-46 in pancreatic cancer models.

Methods

PET scans (1 h post injection) were acquired in PANC-1 xenograft mice (n = 9) after the administration of [^{18}F]FAPI-74 (12.4 ± 1.7 MBq) for the companion imaging. The biodistribution of [^{177}Lu]FAPI-46 was evaluated in the same tumour model (n = 6). For the determination of treatment effects, [^{177}Lu]FAPI-46 and [^{225}Ac]FAPI-46 were injected into PANC-1 xenograft mice with different doses: 3 MBq (n = 6), 10 MBq (n = 6), 30 MBq (n = 6), control (n = 4) for [^{177}Lu]FAPI-46, and 3 kBq (n = 3), 10 kBq (n = 2), 30 kBq (n = 5), control (n = 7) for [^{225}Ac]FAPI-46. Tumour size and body weight were followed.

Results

[^{18}F]FAPI-74 showed rapid clearance via kidneys and high accumulation in the tumour and intestine 1h after administration. [^{177}Lu]FAPI-46 also showed rapid clearance through kidneys and relatively high accumulation in the tumour and large intestine at 24h. Both [^{177}Lu]FAPI-46 and [^{225}Ac]FAPI-46 showed tumour-suppressive effects in a dose-dependent manner, with a mild decrease in body weight. The treatment effects of [^{177}Lu]FAPI-46 were relatively slow but lasted longer than those of [^{225}Ac]FAPI-46.

Conclusion

The dose-dependent tumour-suppressive effect of [^{177}Lu]FAPI-46 and [^{225}Ac]FAPI-46 suggested promising application in FAP-expressing pancreatic cancer.

Introduction

The stroma, which comprises up to 90% of tumour mass, promotes tumour growth, migration, and progression. The fibroblast activation protein (FAP) is highly expressed in cancer-associated fibroblasts (CAFs) of the stroma of many epithelial cancers and is associated with poor prognosis [1–3]. In contrast, low FAP expression is found in normal tissues. Therefore, FAP is an excellent target for the imaging and

therapy. FAP inhibitors (FAPI) are used for theranostics in oncology [4–6]. In previous studies, [^{68}Ga]-labelled FAPI positron emission tomography (PET)/ computed tomography (CT) were proven to be effective in the clinical diagnostics of various cancers [7–9]. [^{99m}Tc]-labelled FAPI derivatives were also synthesized successfully for single photon emission computed tomography imaging [6]. However, reports regarding the therapeutic applications of FAPI are relatively limited. Lindner et al. used [^{90}Y]FAPI-04 for the targeted therapy in a breast cancer patient resulting in pain reduction [10]. Our previous study labelled FAPI-04 with ^{225}Ac, an alpha particle emitter with a half-life of 10 days for its first decay, and investigated the therapeutic effects of [^{225}Ac]FAPI-04 in FAP-expressing human pancreatic cancer [11]. However, FAPI showed rapid excretion via the kidneys, and its biological half-life did not match the physical half-life of ^{225}Ac. Therefore, it is necessary to compare the therapeutic effects of FAPI with improved tumour retention to investigate a better combination of its kinetics and physical decay. In this study, we used ^{177}Lu, a beta emitter with a half-life of 6.7 days, and ^{225}Ac to label FAPI-46 for the targeted therapy and [^{18}F]FAPI-74 PET companion imaging. The purpose of this study was to compare the therapeutic effects of [^{177}Lu]-labelled and [^{225}Ac]-labelled FAPI in FAP-expressing pancreatic cancer xenografts.

Materials And Methods

Preparation of [^{18}F]FAPI-74, [^{177}Lu] and [^{225}Ac]FAPI-46 solutions

The precursor molecules of FAPI-46 and FAPI-74 were obtained from the Heidelberg University based on a material transfer agreement for collaborative research. [^{18}F]FAPI-74 was produced following the methods of previous reports [12]. In short, [^{18}F]fluoride eluted with 0.3 mL of 0.5 M sodium acetate (pH 3.9) was mixed with 0.3 mL of dimethyl sulfoxide (FUJIFILM Wako Pure Chemical, Osaka, Japan) and 6 µL of 10 mM aluminium chloride at room temperature for 5 min. Then, 20 µL of 4 mM FAPI-74 and 4 µL of 20 % ascorbic acid were added, and the fluorination was performed at 95 ^{0}C for 15 min. The mixture was diluted with 10 mL of 0.9 % saline, and [^{18}F]FAPI-74 was captured by passing this diluted solution through a hydrophillic-lipophillic balance cartridge (Waters, Milford, MA). After washing the cartridge with 3 mL of 0.9 % saline, [^{18}F]FAPI-74 was recovered with 0.3 mL of ethanol into a vial containing 2.7 mL of 0.9 % saline.

Lutetium-177 chloride ($^{177}LuCL_3$, 1,110 MBq/mL) dissolved in 0.05 mol/L hydrochloride was purchased from Polatom (Otwock, Poland). Actinium-225 (^{225}Ac) was sourced from the Institute of Material Research at Tohoku University and the Japan Atomic Energy Agency.

[^{177}Lu]FAPI-46 was prepared from the mixture of solutions of 175 µL of 1 mmol/L FAPI-46, 408 µL of 0.3 mole/L sodium acetate, 100 µL of 10w/v% ascorbic acid, and 555 µL of $^{177}LuCL_3$ reacted at 50℃ for 60 minutes.

[^{225}Ac]labelled FAPI-46 was prepared as per the method provided in a previous paper [11]. In brief, a mixture of 300 µL of 1mmol/mL FAPI-46, 100µL of 0.2 mol/L ammonium acetate, 100µL of 7w/v% sodium ascorbate and 200µL of ^{225}Ac solution (300 kBq) were mixed at 80°C for 2 hours.

Preparation of the animals

The human pancreatic cell line, PANC-1, was obtained from the American Type Culture Collection (Manassas, VA, USA). The cells were cultured in RPMI1640 medium with L-glutamine and Phenol Red (FUJIFILM Wako Pure Chemical, Osaka, Japan), supplemented with 10% heat-inactivated fetal bovine serum and 1% penicillin-streptomycin.

Male nude mice were purchased from Japan SLC Inc. (Hamamatsu, Japan). Animals were housed under a 12h light/12h dark cycle and allowed free access to food and water. The mice were injected with PANC-1 cells (1×10^7 cells) in a mixture of phosphate-buffered saline and Matrigel (0.1mL, 1:1; BD Biosciences, Franklin Lakes, NJ, USA).

[^{18}F]FAPI-74 PET imaging and analysis

PET images were acquired with a small animal PET scanner (Siemens Inveon PET/CT) three weeks after the implantation in PANC-1 xenograft mice (9 weeks old, body weight = 25.3 ± 1.2 g, n = 9). Under 2% isoflurane anesthesia, [^{18}F]FAPI-74 (12.4 ± 1.7 MBq) was injected in the tail vein. Dynamic PET scans (scan duration = 70 min, n = 2) and static PET scans (scan duration = 10 min, n = 7) were performed 1 h after injection, followed by a CT scan. PET data were reconstructed into 2-min frames in the dynamic PET scan (2 min × 35 frames) and one frame in the delayed PET scan by three-dimensional ordered-subset expectation-maximization (16 subsets, 2 iterations) with attenuation and scatter correction. Regions of interest were drawn on the muscle, heart, lungs, liver, gallbladder, kidneys, intestine and tumour. The mean standardized uptake values (SUVmean) and maximum standardized uptake values (SUVmax) were measured using PMOD (Version 4.0).

Biodistribution and treatment effect of [^{177}Lu]FAPI-46 in mice

For the evaluation of biodistribution, [^{177}Lu]FAPI-46 (3.3 ± 0.1 MBq) was injected into PANC-1 xenograft mice (9 weeks old, body weight = 23.8 ± 1.1 g, n = 6). After euthanasia by deep inhalation anesthesia of isoflurane, the brain, thyroid gland, salivary gland, lungs, heart, liver, spleen, pancreas, stomach, small intestine, large intestine, kidneys, bone (femur), bladder, testis, tumour, blood, and urine were removed and weighed at 3 h and 24 h. Radioactivity was also measured using a gamma counter (2480 Wizard^2 Gamma Counter, Perkin Elmer, USA).

For the determination of treatment effects, [^{177}Lu]FAPI-46 was injected into PANC-1 xenograft mice via the tail vein (9 weeks old, body weight = 23.5 ± 1.8 g). Mice were divided into four groups according to the injected dose: 3 MBq (3.2 ± 0.1 MBq, n = 6), 10 MBq (10.2 ± 0.5 MBq, n = 6), 30 MBq (30.5 ± 2.7 MBq, n = 6)

and control (n = 4) groups. Tumour size and body weight were measured with a caliper using the elliptical sphere model calculation three times per week for up to 44 days.

Treatment effect of [^{225}Ac]FAPI-46 in the mice

[^{225}Ac]FAPI-46 was injected into PANC-1 xenograft mice via the tail vein (9 weeks old, body weight = 21.7 ± 2.2 g). Mice were divided into four groups according to the injected dose: 3 kBq (2.9 ± 0.0 kBq, n = 3), 10 kBq (8.5 ± 1.1 kBq, n = 2), 30 kBq (30.4 ± 0.7 kBq, n = 5) and control (n = 7) groups. The tumour size and body weight were measured three times per week for up to 32 days.

Immunohistochemistry and histological analysis

All mice were sacrificed after [^{18}F]FAPI-74PET imaging, and tumour xenografts were removed. Immunohistochemical staining was performed using anti-FAP alpha antibody (ab53066; Abcam, Cambridge, UK), and the Dako EnVision + System - HRP Labelled Polymer Anti-Rabbit (K4003) (DAKO Corp., Glostrup, Denmark). To evaluate toxicity, the kidneys were removed after the mice treated with [^{177}Lu]FAPI-46 and [^{225}Ac]FAPI-46 were sacrificed. The tissues were fixed in 10% neutral buffered formalin solution for paraffin blocks and stained with haematoxylin and eosin (H&E). Tumour blocks in all mice were also stained with H&E.

Statistical analysis

Data were expressed as the mean ± standard deviation. Comparisons among the four groups were performed using an unpaired t-test in Microsoft Excel (version 2016) with Bonferroni correction, and $p < 0.05$ were considered statistically significant.

Results

The time-activity curve of the PANC-1 tumour and the normal organs on [^{18}F]FAPI-74 PET are shown in Fig. 1a. [^{18}F]FAPI-74 was cleared rapidly through the kidneys but washout from the tumour occured slow. A static PET image is shown in Fig. 1b. The SUVmean of static scans were 0.24 ± 0.04 in the tumour, 0.05 ± 0.01 in the muscle, 0.08 ± 0.01 in the heart, 0.14 ± 0.02 in the liver, 0.66 ± 0.15 in the gallbladder, 0.61 ± 0.48 in the intestine, and 0.39 ± 0.07 in the kidneys (Fig. 1c). The accumulation in the tumour was significantly higher than most organs at 1h post-injection. Immunohistochemical staining showed FAP expression in the stroma of PANC-1 xenografts (Fig. 2).

The biodistribution of [^{177}Lu]FAPI-46 is shown in Fig. 3. Most organs showed fast clearance between 3h and 24h post-administration, while a relatively high tracer accumulation was seen in the tumour and large intestine at 24h post-injection.

The changes in the tumour size and body weight after administration with [^{177}Lu]FAPI-46 are shown in Fig. 4. Tumour growth showed an inhibitory trend after administration in a dose-dependent manner, although the changes were not statistically significant. The tumour-suppressive effects in the 30 MBq

group were observed 9 days after administration of [^{177}Lu]FAPI-46, while the therapeutic effects in 3 MBq and 10 MBq groups were slower and were seen until day 12. The relative ratio of the tumour size in the 3 MBq, 10 MBq, and 30 MBq groups were 0.62, 0.56, and 0.27 at day 40, respectively, compared to the control group. The body weight in the 10 MBq and 30 MBq groups showed a slight decrease without statistical significance compared to the controls (Fig. 4b).

The results after the administration of [^{225}Ac]FAPI-46 are shown in Fig. 5. The tumour growth was suppressed immediately after treatment in the 10 kBq and 30 kBq groups, while the tumour-suppressive effects in the 3 kBq group were very mild. The tumour size of the 30 kBq groups was significantly smaller than those in the control group on days 5–9 and day 25. The body weight in all the groups showed a decreasing trend in the first week while the 3 kBq and 10 kBq groups showed recovery after day 7.

H&E staining of the tumours and kidneys are shown in Fig. 6. No histological changes were observed in the kidneys of mice injected with [^{177}Lu]FAPI-46 on day 44 and mice injected with [^{225}Ac]FAPI-46 on day 32.

Discussion

The present study showed a rapid clearance of [^{177}Lu]FAPI-46 from normal organs but relatively high accumulation in the PANC-1 tumour model. Dose-dependent tumour-suppressive effects were observed in both PANC-1 xenograft mice treated with [^{177}Lu]FAPI-46 and [^{225}Ac]FAPI-46, respectively. [^{177}Lu]FAPI-46 showed slower but more prolonged therapeutic effects as compared to [^{225}Ac]FAPI-46. We also performed [^{18}F]FAPI-74 PET in PANC-1 xenograft mice and confirmed the high uptake in the tumour as well as the confirmation of FAP expression in the tumour stroma by immunohistochemistry.

We demonstrated the effectiveness of alpha therapy for FAP-expressing pancreatic cancer using [^{225}Ac]FAPI-04 in a previous study [11]. [^{225}Ac]FAPI-04 was thought to irradiate tumour cells by the alpha particles emitted from CAFs in the stoma. However, the alpha irradiation also has affects on CAFs, the primary site of accumulation, which are supporting tumour progression. Since beta particles have a more extended range in tissue compared to alpha particles, beta irradiation may reach tumour cells more homogeneously compared to alpha irradiation. Thus, we used FAPI-46 labelled with ^{177}Lu, a beta emitter, for PANC-1 xenograft mice in the present study. Previous studies reported a rapid internalization of [^{177}Lu]-labelled FAPI derivatives into HT-1080-FAP cells [4] and a high uptake in HT-1080-FAP tumour-bearing mice [4, 13]. In the present study, we also found a relatively high accumulation of [^{177}Lu]FAPI-46 in PANC-1 xenografts, which is considered to target FAP mainly expressed in the stroma. In our previous study, [^{225}Ac]FAPI-04 showed high accumulation in the liver [11], whereas the uptake of [^{177}Lu]FAPI-46 in the liver was low in the experiments presented in this paper. A previous study also reported an increased accumulation of [^{225}Ac]DOTATOC in the liver compared to [^{177}Lu]DOTATOC [14]. The difference was thought to be due to the distribution of free ^{225}Ac since a high uptake of released ^{225}Ac in the liver was found in mice [15], suggesting better *in vivo* stability of [^{177}Lu]FAPI-46.

In the present study, we found that [^{177}Lu]FAPI-46 suppresses tumour growth in a dose-dependent manner. Meanwhile, other beta-emitters, such as ^{90}Y, ^{188}Re, and ^{153}Sm, -labelled with FAPI derivatives were administered in humans without serious side effects [6, 10, 16], suggesting the potential clinical application of [^{177}Lu]FAPI-46. Compared with [^{177}Lu]FAPI-46, [^{225}Ac]FAPI-46 showed faster therapeutic effects in PANC-1 xenograft mice with a shorter duration. The tumour size in mice treated with a high dose of [^{177}Lu]FAPI-46 started to be reduced at 9 days after administration, with a slower growth compared to the control group. In contrast, the tumour growth was reduced immediately after administering a high dose of [^{225}Ac]FAPI-46 while starting to regrow by day 12 with the same tumour growth speed as the control group. However, in a previous study, ^{225}Ac showed a lower survival rate of cells compared to cells treated with ^{177}Lu [17], according to more fatal double-strand breaks induced by alpha particles [18, 19]. Meanwhile, [^{225}Ac]PSMA-617 was effective in metastatic prostate cancer patients refractory to [^{177}Lu]PSMA-617 [20, 21]. We speculate that the reason for the difference seen in our study is due to the fact that the target cells of [^{177}Lu]FAPI-46 and [^{225}Ac]FAPI-46 were CAFs in the stroma as opposed to tumour cells. Stroma cells can tolerate a more fatal environment than other cells and are more radioresistant [22, 23]. However, the effects of alpha irradiation on tumour stromal cells remain to be clarified. Due to a heterogeneous distribution of the stroma and tumour cells causing a heterogeneous dose distribution it might be difficult for alpha particles to reach the tumour cells sufficiently. In contrast, the tumour cells are more likely to be irradiated by beta emission from [^{177}Lu]FAPI-46.

The therapeutic effects of [^{177}Lu]FAPI-46 and [^{225}Ac]FAPI-46 were rather limited, with some of the tumour-suppressive effects being not significant compared to the control group. Since the clearance of FAPI *in vivo* is fast, the biological half-life of FAPI is short, but the physical half-life of ^{177}Lu and ^{225}Ac is relatively long. The unmatched half-life may be the reason for the limited therapeutic effects even with the use of FAPI-46 with improved retention. Radionuclides with a shorter half-life, such as ^{188}Re (half-life = 17.0 h) or ^{211}At (half-life = 7.2 h), maybe better for FAPI therapy by increasing the local dose. Although the procedure for labeling FAPI with ^{211}At has not been established yet, [^{188}Re]-labelled FAPI was synthesized successfully recently and administrated clinically [6]. Therapeutic effects of [^{188}Re]- and [^{211}At]-labelled FAPI should be compared in a future study to investigate these nuclides as more suitable option for FAPI treatment.

Renal toxicity was observed in patients treated with [^{177}Lu]DOTATATE. Renal dysfunction might occur years after [^{177}Lu]DOTATATE therapy, even under kidney protection [24, 25]. However, no histological change was observed in the kidneys after administering [^{177}Lu]FAPI-46 and [^{225}Ac]FAPI-46 in the present study. Although further evaluation should be performed in future studies, our results suggest the clinical feasibility of [^{177}Lu]FAPI-46 and [^{225}Ac]FAPI-46 treatment.

This study had several limitations. First, we used PANC-1 xenograft models with FAP expression in the stroma for the evaluation. However, stroma formation may be different from the tumour stroma in the patients. Therefore, patient-derived xenograft models may ensure in future work a better clinical

translation. Second, the sample size of [^{225}Ac]FAPI-46 was insufficient because of the limited supply of ^{225}Ac. Third, we used radionuclides with a relatively long half-life to target therapy in the pancreatic cancer model. Evaluation of the therapeutic effects using shorter-half-life radionuclides should be further investigated in future studies.

Conclusion

This study revealed dose-dependent therapeutic effects of [^{177}Lu]FAPI-46 and [^{225}Ac]FAPI-46 in PANC-1 xenografts, while the impact of [^{177}Lu]FAPI-46 appeared slow but lasted longer. Beta therapy and alpha therapy targeting FAP can be a promising treatment for pancreatic cancers and needs further evaluation to find the best combination of fast FAP kinetics and physical decay of the radionuclide.

Declarations

Funding

This study was funded by the KAKENHI (B) (Research Number: 19H03602) from the Ministry of Education, Culture, Sports, Science and Technology (MEXT), and the QiSS program of the OPERA (Grant Number: JPMJOP1721) from the Japan Science and Technology Agency (JST), Japan.

Conflict of interest

TL, UH, CK, FLG have a patent application for FAPI-ligands. TL, UH, CK, FLG also hold shares of a consultancy for iTheranostics.

Availability of data and material

Data available on request.

Code availability

Not applicable.

Ethics approval

All experiments were performed in compliance with the guidelines of the Institute of Experimental Animal Sciences. The protocol was approved by the Animal Care and Use Committee of the Osaka University Graduate School of Medicine.

Consent to participate

Not applicable.

Consent for publication

Not applicable.

References

1. Hamson EJ, Keane FM, Tholen S, Schilling O, Gorrell MD. Understanding fibroblast activation protein (FAP): Substrates, activities, expression and targeting for cancer therapy. Proteomics Clin Appl. 2014;8:454–63. https://doi.org/10.1002/prca.201300095.
2. Zi F, He J, He D, Li Y, Yang L, Cai Z. Fibroblast activation protein α in tumor microenvironment: Recent progression and implications [Review]. Mol Med Rep. 2015;11:3203–11. https://doi.org/10.3892/mmr.2015.3197.
3. Wikberg ML, Edin S, Lundberg IV, Van Guelpen B, Dahlin AM, Rutegård J, Stenling R, Öberg Å, Palmqvist R. High intratumoral expression of fibroblast activation protein (FAP) in colon cancer is associated with poorer patient prognosis. Tumour Biol. 2013;34:1013–20. https://doi.org/10.1007/s13277-012-0638-2.
4. Loktev A, Lindner T, Mier W, Debus J, Altmann A, Jäger D, Giesel F, Kratochwil C, Barthe P, Roumestand C, Haberkorn U. A tumor-imaging method targeting cancer-associated fibroblasts. J Nucl Med. 2018;59:1423–9. https://doi.org/10.2967/jnumed.118.210435.
5. Toms J, Kogler J, Maschauer S, Daniel C, Schmidkonz C, Kuwert T, Prante O. Targeting fibroblast activation protein: Radiosynthesis and preclinical evaluation of an ^{18}F-labelled FAP inhibitor. J Nucl Med. 2020;61:1806–13. https://doi.org/10.2967/jnumed.120.242958.
6. Lindner T, Altmann A, Krämer S, Kleist C, Loktev A, Kratochwil C, Giesel F, Mier W, Marme F, Debus J, Haberkorn U. Design and Development of ^{99m}Tc-Labeled FAPI Tracers for SPECT Imaging and ^{188}Re Therapy. J Nucl Med. 2020;61:1507–13. https://doi.org/10.2967/jnumed.119.239731.
7. Giesel FL, Kratochwil C, Lindner T, Marschalek MM, Loktev A, Lehnert W, Debus J, Jäger D, Flechsig P, Altmann A, Mier W. 68Ga-FAPI PET/CT: Biodistribution and preliminary dosimetry estimate of 2 DOTA-containing FAP-targeting agents in patients with various cancers. J Nucl Med. 2019;60:386–92. https://doi.org/10.2967/jnumed.118.215913.
8. Kratochwil C, Flechsig P, Lindner T, Abderrahim L, Altmann A, Mier W, Adeberg S, Rathke H, Röhrich M, Winter H, Plinkert PK. 68Ga-FAPI PET/CT: Tracer uptake in 28 different kinds of cancer. J Nucl Med. 2019;60:801–5. https://doi.org/10.2967/jnumed.119.227967.
9. Meyer C, Dahlbom M, Lindner T, Vauclin S, Mona C, Slavik R, Czernin J, Haberkorn U, Calais J. Radiation dosimetry and biodistribution of (68)GaFAPI-46 PET imaging in cancer patients. J Nucl Med. 2020;61:1171–7. https://doi.org/10.2967/jnumed.119.236786.
10. Lindner T, Loktev A, Altmann A, Giesel F, Kratochwil C, Debus J, Jäger D, Mier W, Haberkorn U. Development of quinoline-based theranostic ligands for the targeting of fibroblast activation protein. J Nucl Med. 2018;59:1415–22. https://doi.org/10.2967/jnumed.118.210443.
11. Watabe T, Liu Y, Kaneda-Nakashima K, Shirakami Y, Lindner T, Ooe K, Toyoshima A, Nagata K, Shimosegawa E, Haberkorn U, Kratochwil C. Theranostics targeting fibroblast activation protein in

the tumor stroma: (64)Cu- and (225)Ac-Labelled FAPI-04 in pancreatic cancer xenograft mouse models. J Nucl Med. 2020;61:563–9. https://doi.org/10.2967/jnumed.119.233122.

12. Giesel FL, Adeberg S, Syed M, Lindner T, Jiménez-Franco LD, Mavriopoulou E, Staudinger F, Tonndorf-Martini E, Regnery S, Rieken S, El Shafie R FAPI-74 PET/CT using either (18)F-AlF or cold-kit (68)ga labeling: biodistribution, radiation dosimetry, and tumor delineation in lung cancer patients. J Nucl Med. 2021;62:201–7. https://doi.org/10.2967/jnumed.120.245084.
13. Loktev A, Lindner T, Burger EM, Altmann A, Giesel F, Kratochwil C, Debus J, Marmé F, Jäger D, Mier W, Haberkorn U. Development of fibroblast activation protein-targeted radiotracers with improved tumor retention. J Nucl Med. 2019;60:1421–9. https://doi.org/10.2967/jnumed.118.224469.
14. Miederer M, Henriksen G, Alke A, Mossbrugger I, Quintanilla-Martinez L, Senekowitsch-Schmidtke R, Essler M. Preclinical evaluation of the alpha-particle generator nuclide 225Ac for somatostatin receptor radiotherapy of neuroendocrine tumors. Clin Cancer Res. 2008;14:3555–61. https://doi.org/10.1158/1078-0432.ccr-07-4647.
15. Miederer M, Scheinberg DA, McDevitt MR. Realizing the potential of the actinium-225 radionuclide generator in targeted alpha particle therapy applications. Adv Drug Deliv Rev. 2008;60:1371–82. https://doi.org/10.1016/j.addr.2008.04.009.
16. Kratochwil C, Giesel FL, Rathke H, Fink R, Dendl K, Debus J, Mier W, Jäger D, Lindner T, Haberkorn U. [^{153}Sm]Samarium-labelled FAPI-46 radioligand therapy in a patient with lung metastases of a sarcoma. Eur J Nucl Med Mol Imaging. 2021; 17:1–3. https://doi.org/10.1007/s00259-021-05273-8.
17. Nayak T, Norenberg J, Anderson T, Atcher R. A comparison of high- versus low-linear energy transfer somatostatin receptor targeted radionuclide therapy in vitro. Cancer Biother Radiopharm. 2005;20:52–7. https://doi.org/10.1089/cbr.2005.20.52.
18. Lyckesvärd MN, Delle U, Kahu H, Lindegren S, Jensen H, Bäck T, Swanpalmer J, Elmroth K. Alpha particle induced DNA damage and repair in normal cultured thyrocytes of different proliferation status. Mutat Res. 2014;765:48–56. https://doi.org/10.1016/j.mrfmmm.2014.04.005.
19. Lorat Y, Timm S, Jakob B, Taucher-Scholz G, Rübe CE. Clustered double-strand breaks in heterochromatin perturb DNA repair after high linear energy transfer irradiation. Radiother Oncol. 2016;121:154–61. https://doi.org/10.1016/j.radonc.2016.08.028.
20. Kratochwil C, Bruchertseifer F, Rathke H, Bronzel M, Apostolidis C, Weichert W, Haberkorn U, Giesel FL, Morgenstern A. Targeted alpha-therapy of metastatic castration-resistant prostate cancer with ^{225}Ac-PSMA-617: dosimetry estimate and empiric dose finding. J Nucl Med. 2017;58:1624–31. https://doi.org/10.2967/jnumed.117.191395.
21. Feuerecker B, Tauber R, Knorr K, Heck M, Beheshti A, Seidl C, Bruchertseifer F, Pickhard A, Gafita A, Kratochwil C, Retz M. Activity and adverse events of actinium-225-PSMA-617 in advanced metastatic castration-resistant prostate cancer after failure of lutetium-177-PSMA. Eur Urol. 2021;79:343–50. https://doi.org/10.1016/j.eururo.2020.11.013.
22. Wang Z, Tang Y, Tan Y, Wei Q, Yu W. Cancer-associated fibroblasts in radiotherapy: Challenges and new opportunities. Cell Commun Signal. 2019;17:47. https://doi.org/10.1186/s12964-019-0362-2.

23. Domogauer JD, de Toledo SM, Howell RW, Azzam EI. Acquired radioresistance in cancer associated fibroblasts is concomitant with enhanced antioxidant potential and DNA repair capacity. Cell Commun Signal. 2021;19:30. https://doi.org/10.21203/rs.3.rs-115117/v1.
24. Bodei L, Cremonesi M, Ferrari M, Pacifici M, Grana CM, Bartolomei M, Baio SM, Sansovini M, Paganelli G. Long-term evaluation of renal toxicity after peptide receptor radionuclide therapy with 90Y-DOTATOC and 177Lu-DOTATATE: The role of associated risk factors. Eur J Nucl Med Mol Imaging. 2008;35:1847–56. https://doi.org/10.1007/s00259-008-0778-1.
25. Gupta SK, Singla S, Bal C. Renal and hematological toxicity in patients of neuroendocrine tumors after peptide receptor radionuclide therapy with 177Lu-DOTATATE. Cancer Biother Radiopharm. 2012;27:593–9. https://doi.org/10.1007/s00259-008-0778-1.

Figures

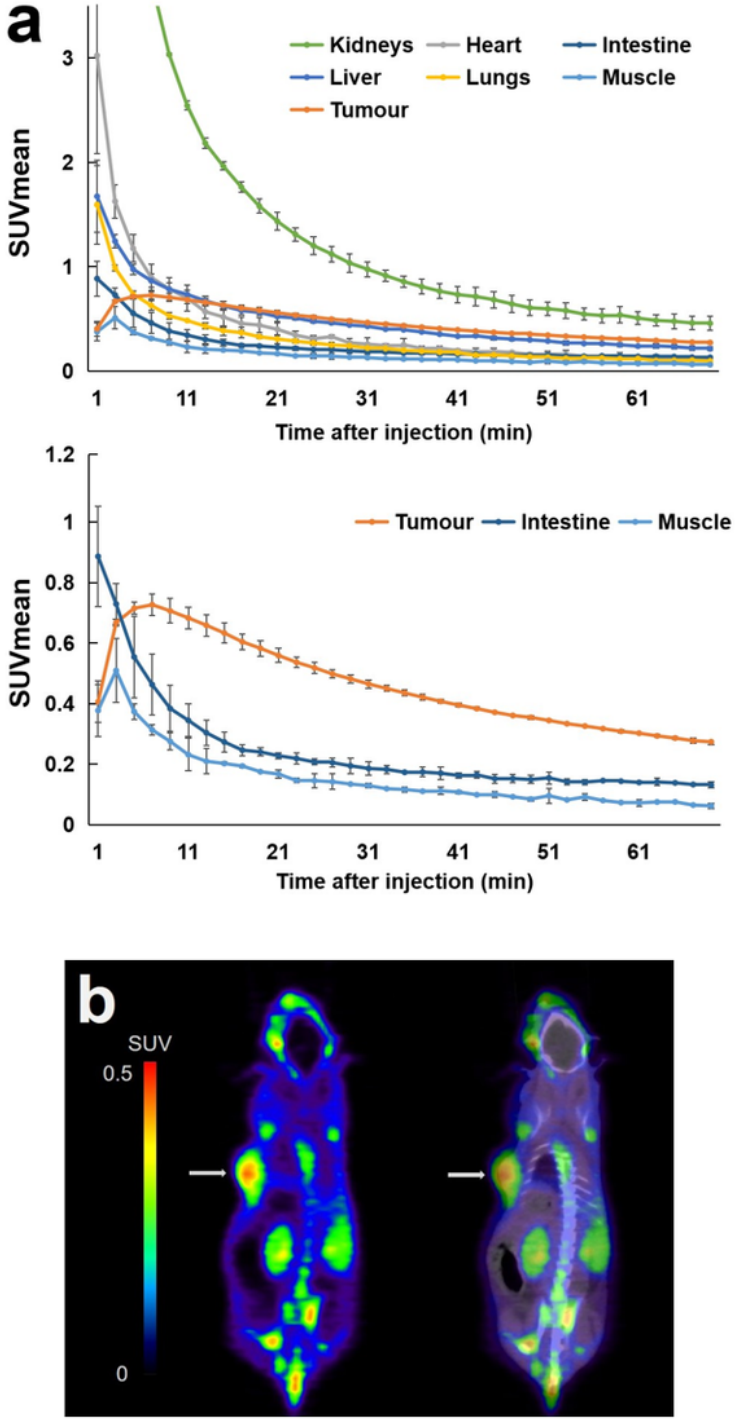

Figure 1

(a) Time-activity curves of [18F]FAPI-74 in PANC-1 tumour and normal organs. (b) Static coronal PET imaging (left) and PET/CT fusion imaging (right) of [18F]FAPI-74 (1-h post-administration) in PANC-1 xenograft mice. Arrows revealed tumour xenograft on the left side. (c) The SUVmean (upper) and SUVmax (lower) in the tumour and normal organs. The high uptake by the gallbladder and kidneys was due to the excretion through bile and urine.

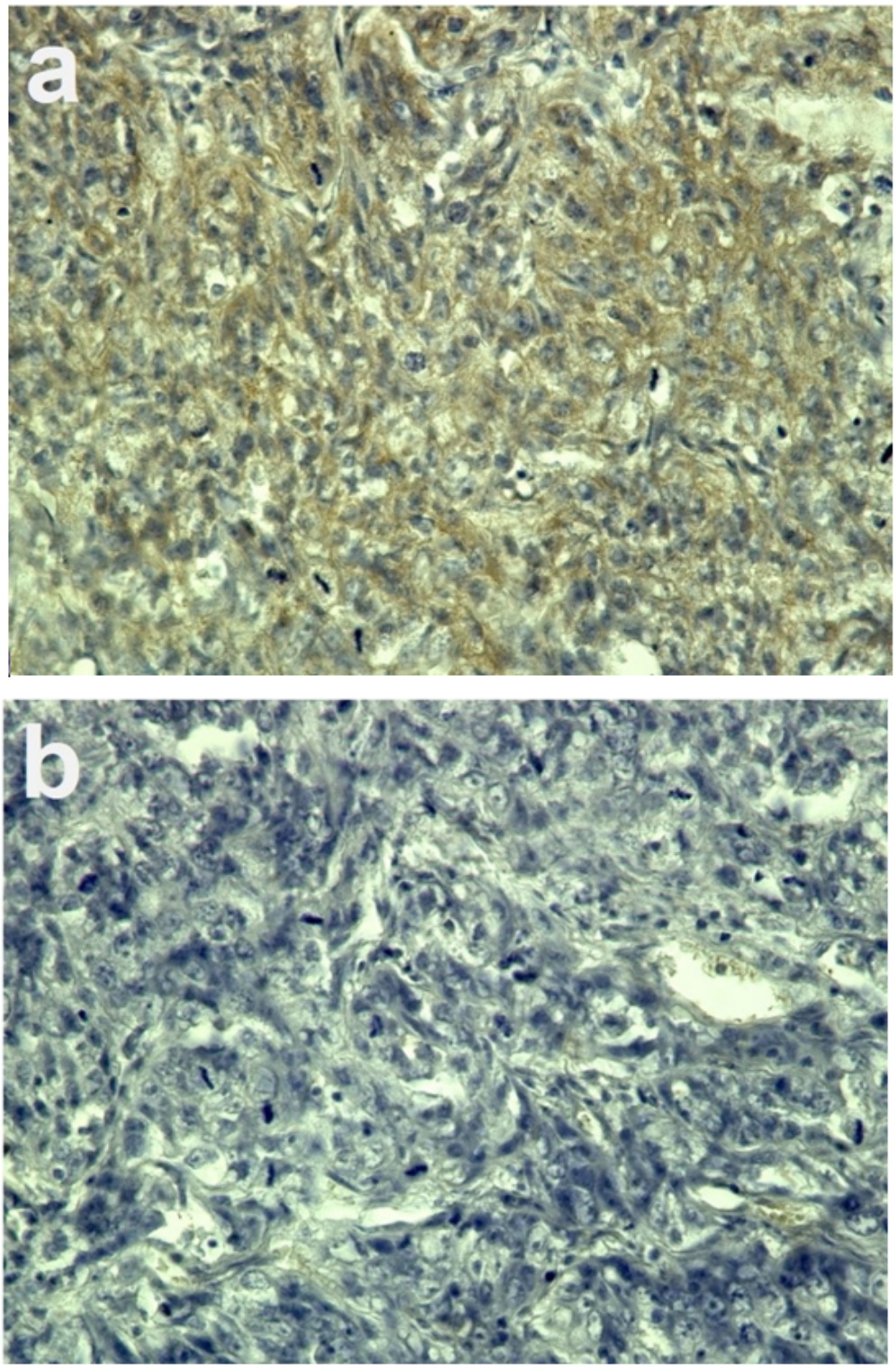

Figure 2

(a) Immunohistochemical staining of fibroblast activation protein (FAP) in PANC-1 xenograft and (b) negative control without primary antibody (magnification ×400). FAP expression was observed in the tumour stroma.

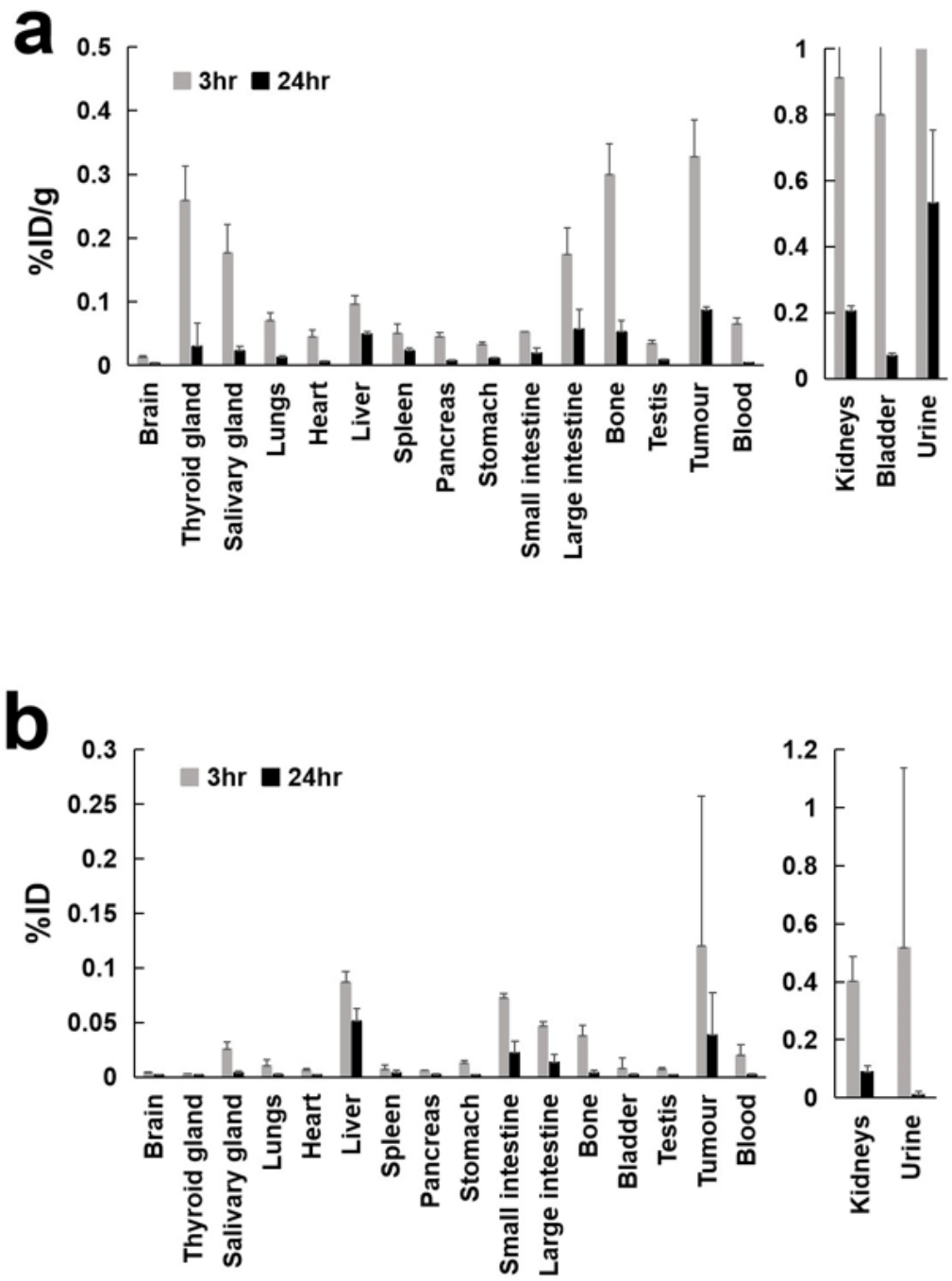

Figure 3

The %ID/g (a) and %ID (b) of [177Lu]FAPI-46 in the PANC-1 xenograft mice at 3h and 24h post-administration. (%ID/g of the urine was 21.2 ± 15.3 % at 3hr post-administration.)

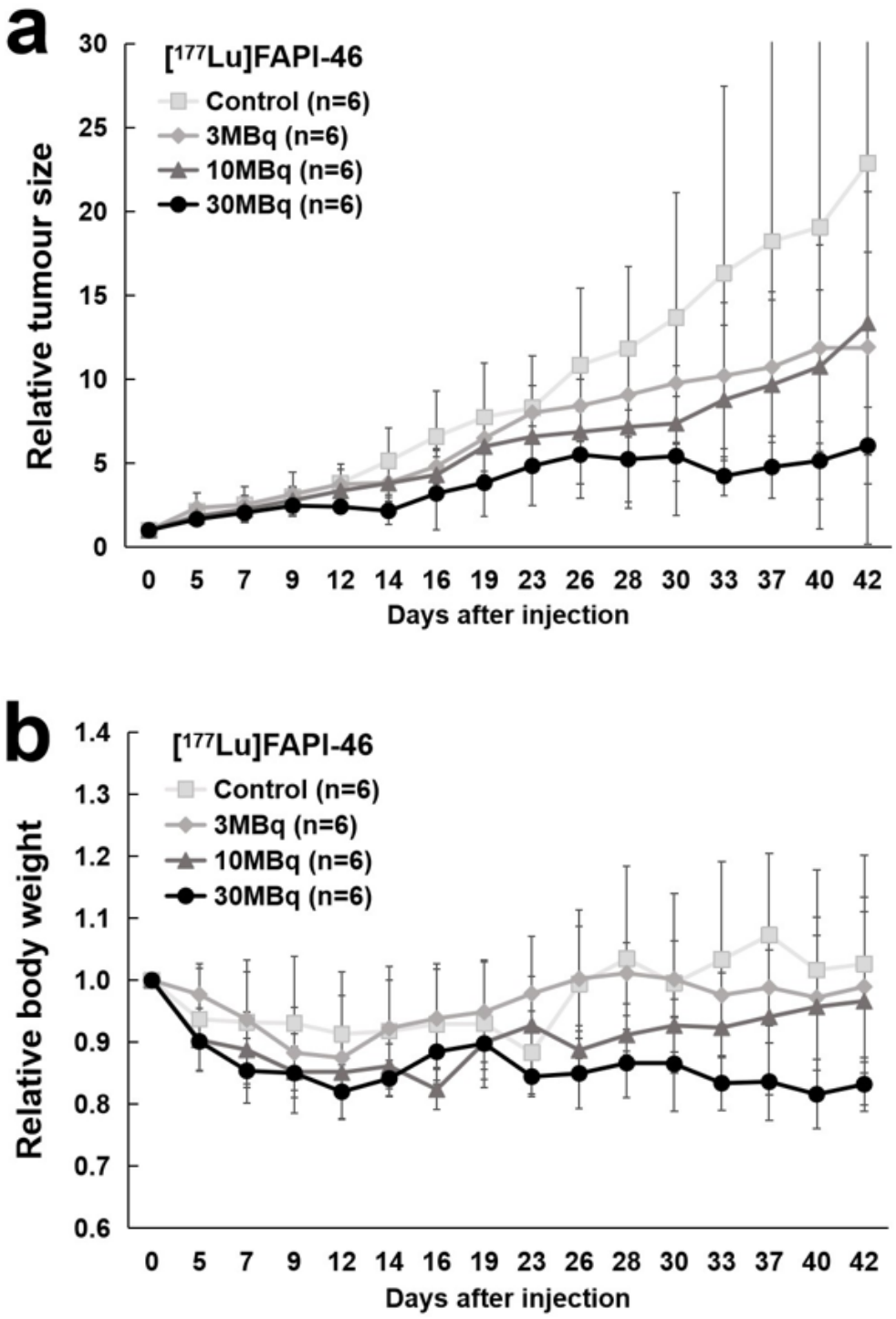

Figure 4

Changes in the relative tumour size (a) and the relative body weight (b) in PANC-1 xenograft mice treated with [177Lu]FAPI-46.

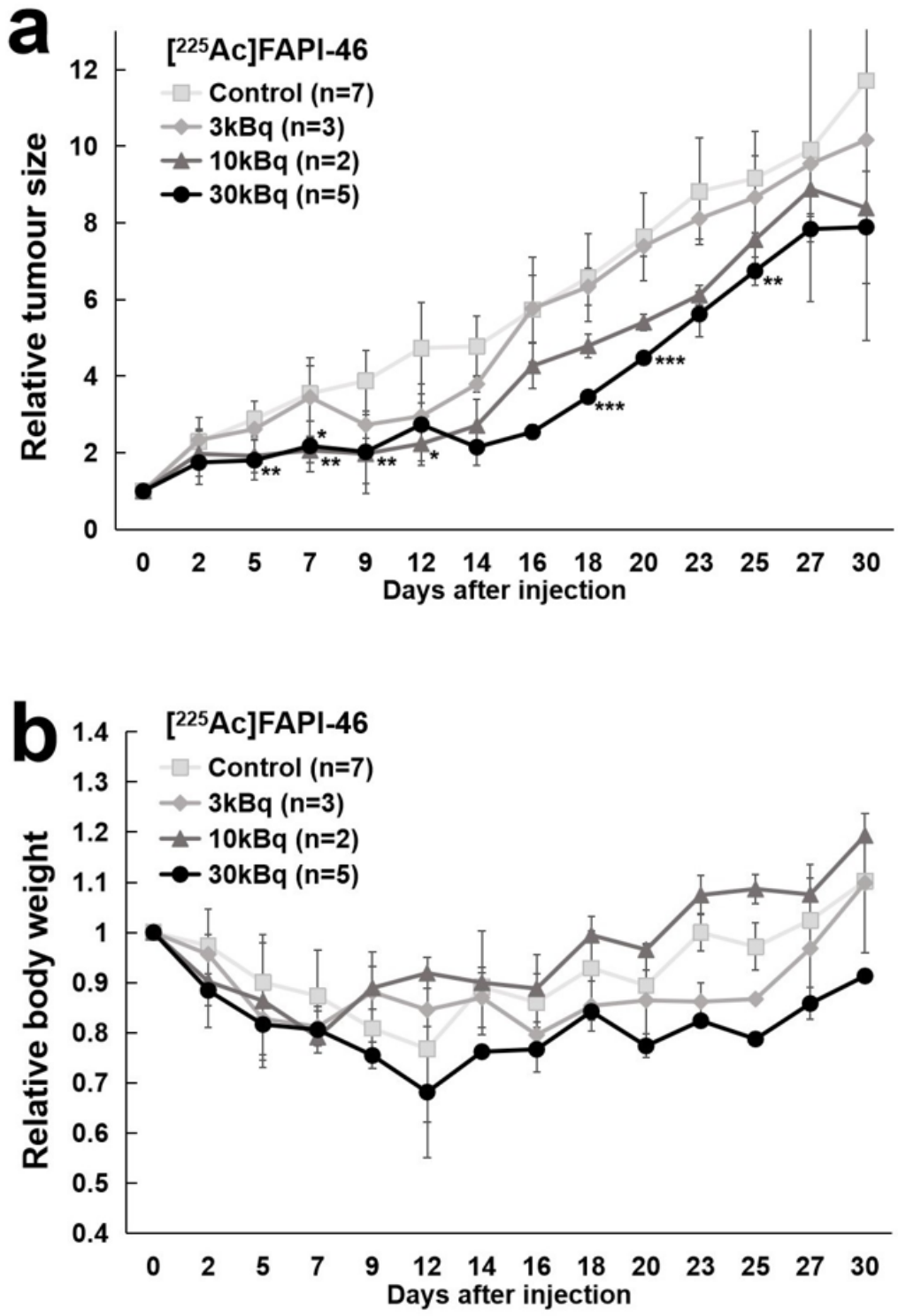

Figure 5

Changes of the relative tumour size (a) and the relative body weight (b) in PANC-1 xenograft mice treated with [225Ac]FAPI-46. (*p<0.05 between 10 kBq and control group; **p<0.05 between 30 kBq and control group; ***p<0.05 between 3 kBq and 30 kBq group.)

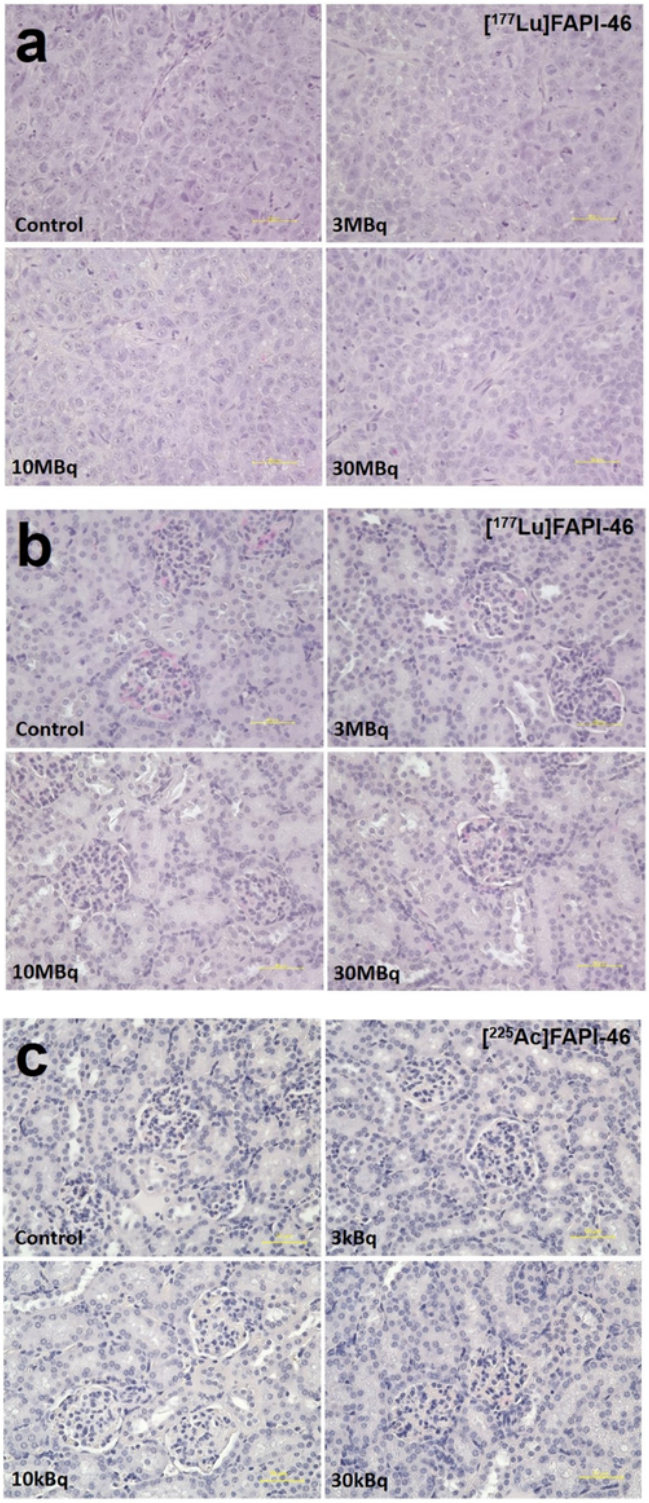

Figure 6

Histological changes evaluated by haematoxylin and eosin staining in the tumour (a) and the kidney (b) at day 44 after the administration of [177Lu]FAPI-46, and the kidney (c) at day 32 after the administration of [225Ac]FAPI-46. No significant difference was observed both in the tumour and the kidney. Yellow bar indicates 50μm.